

Superconducting Diode Effect in Two-dimensional Topological Insulator Edges and Josephson Junctions

H. Huang,¹ T. de Picoli,¹ and J. I. Väyrynen¹

Department of Physics and Astronomy, Purdue University, West Lafayette, Indiana 47907 USA

(Dated: 24 April 2024)

The superconducting diode effect – the dependence of critical current on its direction – can arise from the simultaneous breaking of inversion and time-reversal symmetry in a superconductor and has gained interest for its potential applications in superconducting electronics. In this letter, we study the effect in a two-dimensional topological insulator (2D TI) in both a uniform geometry as well as in a long Josephson junction. We show that in the presence of Zeeman fields, a circulating edge current enables a large non-reciprocity of the critical current. We find a maximum diode efficiency 1 for the uniform 2D TI and $(\sqrt{2} - 1)^2 \approx 0.17$ for the long Josephson junction.

In a superconductor with broken inversion and time-reversal symmetry, the critical current can depend on the direction of the current bias, an effect known as the superconducting diode effect (SDE)^{1,2}. Although the phenomenon is not new^{3–5}, the subject has attracted renewed interest after the suggestion that the effect might be intrinsic to some materials^{6–27} as opposed to of extrinsic geometric nature^{3,25,28–36}. The effect can be realized in critical current of both uniform (junctionless) systems^{3–8,10–12,18,20–22,24,27,30–33,37,38} as well as Josephson junctions^{9,13–17,23,25,34–36,39–43}, but the relation of the two diode effects has not been completely clear.

A widely studied mechanism for inversion symmetry breaking in an intrinsic SDE is strong spin-orbit coupling^{8,11,12,20,21,23,26,40,43–45}. A prime example displaying the effects of strong spin-orbit coupling is the time-reversal symmetric two-dimensional topological insulator (2D TI)^{46–49}. These systems have been also studied in the superconducting state, see for example HgTe^{50–52} or monolayer 1T' WTe₂^{53–55}.

Diode effect and related non-reciprocal effects have been theoretically proposed in 2D TI Josephson junctions^{39,56–59}, mostly in the short junction limit (junction length less than superconducting coherence length). In this paper, we show that a *uniform* 2D TI edge can display a large diode effect in its critical current, when the current is limited by Cooper pair depairing²¹. We then show an analogous Josephson diode effect in a long Josephson junction. We attribute both diode effects to the same mechanism that is unique to 2D TI edge: a circulating current generated by Zeeman field or magnetization.

Two-dimensional topological insulator has an insulating bulk gap but gapless helical (spin-momentum locked) one-dimensional boundary modes. The low-energy Hamiltonian for a single helical edge state is

$$H_{\text{helical edge}} = v\hat{p}_x\sigma_z + \sum_{i=x,y,z} V_i\sigma_i, \quad (1)$$

where v is the edge mode Dirac velocity, $\hat{p}_x = -i\hbar\partial_x$ is the momentum operator and $\sigma_{x,y,z}$ the spin Pauli matrices; we choose the helical edge spin quantization axis to be the z -axis. We also include a magnetic perturbation V_i that breaks time-reversal symmetry of the edge and allows the system to present the diode effect. The term V_i may arise from Zeeman coupling to magnetic field as $V_i = \frac{1}{2}g\mu_B B_i$ or from exchange coupling to a magnetic material; for concreteness we call this a Zeeman field in the rest of the article. A perpendicular

Zeeman field V_i (e.g., in the x -direction) opens a gap in the edge dispersion, whereas a field along the spin quantization axis, V_z , merely polarizes the edge and shifts the Dirac point position, see Fig. 1a. In a finite system V_z will therefore induce a circulating current along the boundary of the system⁵⁷. This current will lead to various non-reciprocal effects, previously mostly studied in Josephson junctions^{56,60}. Here, we first show a large superconducting diode effect in the absence of a junction and then discuss diode effect in a long Josephson junction.

Because the edge Hamiltonian consists of counterpropagating states with opposite spins, conventional singlet s-wave superconductivity can be induced. In the presence of a supercurrent and a Zeeman field along z , the (2nd quantized) Hamiltonian of a single proximitized 2D TI edge is given by $\mathcal{H} = \frac{1}{2} \int dx \Psi^\dagger(x) H(x, q) \Psi(x)$,

$$H(x, q) = (v\hat{p}_x\sigma_z - \mu)\tau_z + V_z\sigma_z + \Delta e^{iqx}\tau_x, \quad (2)$$

where μ is the chemical potential, Δ the induced gap, and q the Cooper pair momentum that models an externally applied supercurrent $I_w = ev\hbar q$. We will consider here the zero temperature limit where many of the calculations can be done analytically. The Hamiltonian acts on the Nambu spinor $\Psi(x) = (\psi_\uparrow, \psi_\downarrow, \psi_\downarrow^\dagger, -\psi_\uparrow^\dagger)^T$ with $\tau_{x,y,z}$ Pauli matrices acting on the particle-hole space. We note that the spatial modulation of the pairing term gives rise to an effective Zeeman term $\tilde{V}_z = V_z + \frac{1}{2}v\hbar q$ by taking a unitary transformation into a moving frame $\tilde{H}(x, q) = e^{-iqx\tau_z/2} H(x, q) e^{iqx\tau_z/2}$. At the same time, the gap to quasiparticle excitations vanishes at a critical Zeeman energy $\tilde{V}_{z,c} = \pm\Delta$ which also gives the critical Cooper pair momentum $|q_c| = \Delta/(\frac{1}{2}\hbar v)$ at zero magnetic field²¹. At a non-zero magnetic field, the above expression predicts critical Cooper pair momenta $q_c^\pm = (\pm\Delta - V_z)/(\frac{1}{2}\hbar v)$, with a gapped superconducting state in the interval $q_c^-(V_z) < q < q_c^+(V_z)$. Remarkably, the current created by V_z opposite to q enables a superconducting state even at large Zeeman field and applied currents as well as leads to a large diode effect on the edge, see Fig. 1c. The diode efficiency $\eta = (|q_c^+| - |q_c^-|)/(|q_c^+| + |q_c^-|)$ becomes 1 when $V_z = \pm\Delta$ and the critical current in one direction vanishes, $q_c^\pm = 0$.

The helicity of the helical edge can be reversed by setting $v \rightarrow -v$ in Eq. (2). In a system with two otherwise *identical* topological insulator edges of opposite helicities, Fig. 1b, the

diode effect vanishes since the combined system is inversion symmetric, Fig. 1c. By breaking the symmetry between the two edges one can recover the diode effect^{21,39,59}, analogous to an asymmetric ring³¹; In Fig. 1b we break the symmetry by assuming unequal induced gaps $\Delta_{1,2}$ for the two edges.

The linearized description, Eq. (2), is valid near the Fermi level at energies much below the bulk band gap E_g of the 2D topological insulator. One might therefore wonder if the large diode effect described above is an artifact of the linearized low-energy approximation. To answer this question, we simulate a 2D TI Hamiltonian in a ribbon geometry (Fig. 1b) by using a tight-binding model. Specifically, we discretize the BHZ model⁴⁶ using Kwant⁶¹ python package⁶². While the original model⁴⁶ was for a HgTe quantum well, we use model parameters that make simulations computationally cheaper but still belong to the same topological phase. In our model, we consider two different chemical potentials $\mu = -0.149E_g$ and $-0.484E_g$ (measured from the Dirac point) corresponding to superconducting coherence lengths (v_F denotes the Fermi velocity) $\hbar v_F/\Delta \approx 40a$ and $21a$, respectively, in units of the lattice constant a , and observe no qualitative difference in the results. In the remaining of this article, we show the results for the second case. The ribbon width $L_y = 80a$ is chosen to be much larger than the edge penetration depth $\hbar v/E_g \approx 0.56a$, and so that the two edges do not couple to each other.

We find numerically the values of q at which the gap to quasiparticle excitation closes. The resulting critical momenta q_c^\pm vs V_z are shown in Fig. 1c, where we consider three cases: (i) $\Delta_1 = \Delta_2 = \Delta$, (ii) $\Delta_1 = \Delta$, $\Delta_2 = 5\Delta_1$, and (iii) $\Delta_1 = \Delta/2$, $\Delta_2 = 5\Delta_1$, with $\Delta/E_g = 0.0134$. In case (i), the system is inversion symmetric and shows no diode effect, while in case (ii) and (iii), we observe diode effects. To identify which edge becomes normal at $q = q_c$, we also investigate the probability densities of the zero-energy gapless quasiparticle state at the SC/N phase boundary. At boundaries with negative slopes in V_z - q_c plane, the lower edge of the ribbon turns normal. The upper edge becomes normal at the boundaries with positive slopes in cases (i) and (iii). These observations are expected from the low-energy model, Eq. (2). However, in case (ii) which has a larger Δ than case (iii), we observe that the gapless quasiparticle states at the positive-slope boundary have a non-zero probability density in the bulk region of the ribbon, and as a consequence, the slope of the boundary is different from those due to edge states. This is not predicted by the lower-energy model. We note that for our choice of μ , the valence band edge is only a distance $0.04E_g \approx 3\Delta$ from the Fermi level in this case.

Next, we study non-reciprocity in a 2D TI Josephson junction, depicted in Fig. 2a. We consider a junction of width W where the two superconductors have a phase difference ϕ . To break inversion and time-reversal symmetry we consider a magnetic field-induced Zeeman energy in the junction. The bottom half of the junction at $-\frac{W}{2} < x < \frac{W}{2}$ can be therefore described by the effective Hamiltonian (2) with the replacements $V_z\sigma_z \rightarrow \Theta(\frac{W}{2} - |x|)V_i\sigma_i$ ($i = x, z$) and

$$\Delta e^{iqx\tau_z}\tau_x \rightarrow \text{Re}[\Delta(x)]\tau_x - \text{Im}[\Delta(x)]\tau_y, \quad (3)$$

where $\Delta(x) = \Theta(|x| - \frac{W}{2})\Delta_0 e^{i\phi(x)}$ and $\phi(x) = \Theta(x - \frac{W}{2})\phi$.

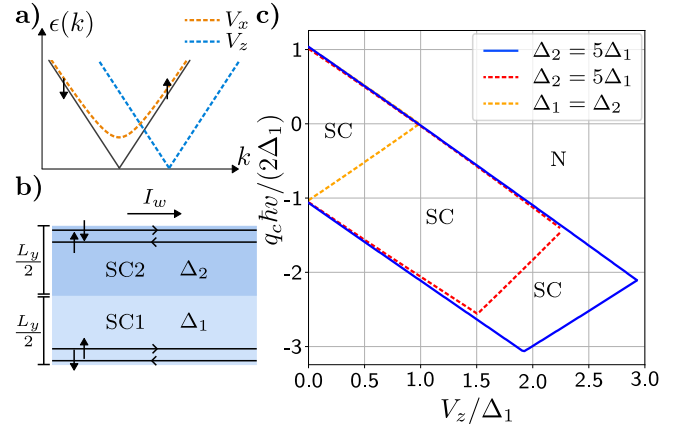


FIG. 1: Superconducting diode effect in the critical current of a uniform (junctionless) 2D topological insulator ribbon.

a) Effect of a Zeeman field on the single edge dispersion. A field perpendicular to the spin quantization axis (which we choose to be z axis) opens a gap in the dispersion, while a field along the spin quantization axis shifts the Dirac point momentum. b) Geometry of the ribbon in our numerical model. The superconducting gap of the lower and upper half of the ribbon are Δ_1 and Δ_2 , respectively, to break inversion symmetry. c) Critical momenta q_c^\pm versus V_z for the ribbon, where only the $V_z \geq 0$ part is shown since $q_c^\pm(V_z) = -q_c^\mp(-V_z)$. The dashed lines are obtained for $\Delta_1 = \Delta$ and the solid line is for $\Delta_1 = \Delta/2$. For $\Delta_2 = 5\Delta_1$, we achieve diode efficiency $\eta = 1$ at $V_z = \Delta_1$ as q_c^+ vanishes. Along the solid boundary, the quasiparticle gap closes on one of the edges of the system. In the case of larger gap, $\Delta_1 = \Delta, \Delta_2 = 5\Delta_1$ (the red dashed line), the size of the superconducting phase is limited by bulk states: the positive-slope boundary is due to gapless bulk states as opposed to edge states in other cases. Our numerical results indicate that $|q_c^\pm(V_z = 0)| \approx 2\Delta_1/(\hbar v)$ is determined by the Dirac velocity v , thus approximately independent of μ .

For each value of the Josephson phase ϕ , the system has a set of energy eigenvalues $E(\phi)$. The zero-temperature Josephson current of the junction is defined as⁶³

$$I_J(\phi) = \frac{2e}{\hbar} \frac{dE_{\text{GS}}(\phi)}{d\phi}. \quad (4)$$

Here E_{GS} is the ground state energy of the corresponding many-body system, which can be written as the sum of all negative energy eigenvalues $\{E_i^-(\phi)\}$ of our single-electron system:

$$E_{\text{GS}}(\phi) = \sum_{i=1}^{\infty} E_i^-(\phi). \quad (5)$$

We numerically study $E_{\text{GS}}(\phi)$ and $I_J(\phi)$ of the junction depicted in Fig. 2a. In our tight-binding simulation we model a 2D $L_x \times L_y$ system with $L_x = 120a$, $L_y = 80a$, $W = 40a$, and $\xi = 21a$. The Zeeman fields in the junction are applied to rectangular regions of size $W \times d$ with $d = 10a$ chosen to be much larger than the edge penetration depth.

We calculated the Josephson current in various combinations of Zeeman potentials V_z or V_x applied to the two edges. Since L_y is much larger than the edge penetration depth, the current can be understood as the sum of two contributions, from the upper and lower edge:

$$I_J(\phi) = I_{J,\text{upper}}(\phi) + I_{J,\text{lower}}(\phi), \quad (6)$$

and the effect of applying magnetic fields to the edges on $I_J(\phi)$ can be understood in terms of these single-edge contributions.

We consider the limit of a long junction $W \gtrsim \xi$, where the Josephson current $I_J(\phi)$ is a piecewise linear function⁶⁴ as are its single-edge contributions in Eq. (6). We can model each term with a 2π -periodic piece-wise linear function⁵⁶:

$$I_{J,\text{single edge}}(\phi) \approx \begin{cases} \frac{I_0}{\pi-t}\phi & \text{if } \phi \bmod 2\pi \in [0, \pi-t) \\ -\frac{I_0}{t}(\phi - \pi) & \text{if } \phi \bmod 2\pi \in [\pi-t, \pi+t) \\ \frac{I_0}{\pi-t}(\phi - 2\pi) & \text{if } \phi \bmod 2\pi \in [\pi+t, 2\pi), \end{cases} \quad (7)$$

where I_0 is the maximum single edge Josephson current and $\pi \pm t$ are the ϕ values at which $I_{J,\text{single edge}}(\phi)$ reaches minimum and maximum, respectively. Matching Eq. (7) with our numerically calculated Josephson currents, we find $t \approx 0.0659$.

Next, we describe the effects of V_x and V_z on a single edge Josephson current. Applying a magnetic field V_x perpendicular to the spin quantization axis on an edge gaps the Dirac point (Fig. 1a) and lowers the transmission of the edge state⁶⁵. Thus, V_x will have the effect of flattening the phase dispersion of Andreev states and thus suppressing the Josephson current, see Fig. 2b-c.

On the other hand, applying a V_z field on an edge only shifts the Andreev state energies in ϕ and consequently the Josephson current is shifted in ϕ while its maximum value does not change (Fig. 2b-c). Thus, with V_z one can realize a ϕ_0 junction⁵⁶. In particular, we find that for values of V_z where linearized model is valid ($V_z < |E_g - \mu|$), the shift $\Delta\phi$ of these curves in ϕ is linear,

$$\Delta\phi = c \frac{V_z}{\Delta_0} \text{ for } V_z < |E_g - \mu|, \quad (8)$$

where c is a unit-free constant, estimated below, see Eq. (10). Since the Josephson current of a long junction is (piecewise) linear in ϕ , the result Eq. (8) is analogous to the Zeeman induced current on the helical edge, discussed below Eq. (1), with the exception that the Josephson current is a 2π -periodic function of ϕ .

The prefactor c in Eq. (8) can be estimated based on the low-energy model (2). The energy of the lowest Andreev bound state on the lower edge under zero field is⁶⁶

$$E_1(\phi) = \frac{1}{2} E_T \frac{W}{W + \xi} |\phi - \pi|, \quad (9)$$

which, upon taking the Thouless energy $E_T = \hbar v/W \approx 0.525\Delta_0$ and $W = 1.904\xi$ (so that $E_1(\phi = 0) = 0.541\Delta_0$) matches well with the numerically calculated result, see Fig. 2b. Higher-energy Andreev states have similar expressions⁶⁶. The Andreev state is a $\sigma_z = \sigma = \pm 1$ eigenstate whose

wave function extends a distance ξ into the superconducting banks. Therefore, a Zeeman field V_z in the junction shifts its energy by approximately $V_z \times W/(W + \xi)$ which in Eq. (9) can be compensated by shifting ϕ by the amount given in Eq. (8) with a proportionality constant

$$c \approx \sigma \frac{2W}{\xi} \approx 3.81\sigma, \quad (10)$$

which is on the same order of magnitude as a numerically obtained value of 3.57 ± 0.03 . Here $\sigma = \pm 1$ depending on the helicity of the edge. Thus the shift $\Delta\phi$, Eq. (8), is opposite on two edges of a junction with same V_z .

Next, we will investigate the effect of combined V_x, V_z terms on the two edges of the junction, focusing on the Josephson diode effect. We define Josephson diode efficiency

$$\eta_J = |I_{J,c}^+ + I_{J,c}^-| / |I_{J,c}^+ - I_{J,c}^-|, \quad (11)$$

via the maximum and minimum Josephson currents (critical currents), respectively $I_{J,c}^+ = \max_\phi I_J$ and $I_{J,c}^- = \min_\phi I_J$, obtained from Eq. (6).

When the junction is inversion symmetric, such as in the case of applying a symmetric V_z field on both edges, we have $\eta_J = 0$. By applying a symmetric V_z on both edges, the $E_i(\phi)$ curves of the upper and lower edge states and their contributions to the Josephson current are shifted by the same amount in ϕ , but in opposite directions, see Fig. 2b-c and Eq. (10). The ground state energy (Josephson potential) has two inequivalent minima, but each minimum is symmetric and therefore the critical current shows no diode effect, see Fig. 3c⁶⁷. Asymmetrically applied V_z can be symmetrized by an appropriate shift of ϕ , without changing the Josephson critical current. Thus, there is no diode effect in a long junction with only V_z , even if applied asymmetrically. This agrees with small magnetization limit of Ref. 59. However, they found a non-zero diode effect in a short junction with large magnetization where Eq. (8) might not hold.

By applying V_x on one edge, we can break inversion symmetry. However, without V_z , the Josephson current (6) can be again symmetrized and will have no diode effect. Diode effect requires both V_x and V_z in an inversion-symmetry breaking way. Such combination leads to an asymmetric Josephson potential and non-reciprocal critical currents, see Fig. 3a-b. With certain combinations of V_x and V_z , the Josephson potential will have two stable minima, see Fig. 3a. If one can initialize the phase of the junction into one of the stable minima ϕ_* , the effective critical currents of the system will be the two extrema of the Josephson current nearest to ϕ_* ^{28,68}. The difference between the two critical currents in such cases can be large, as in Fig. 3a, even if the “global” diode efficiency (11) is small.

For a zero-temperature long Josephson junction, where Eqs. (6) and (7) hold, the diode efficiency (11) can be calculated analytically. In Fig. 4 we show the effect of V_x on one edge and V_z on the other on the diode efficiency η_J .

In summary, we have shown that by applying Zeeman fields to the edges of a 2D TI, one can achieve a large non-reciprocal critical current. Specifically, for a uniform 2D TI edge, the maximum diode efficiency is 1. For a zero-

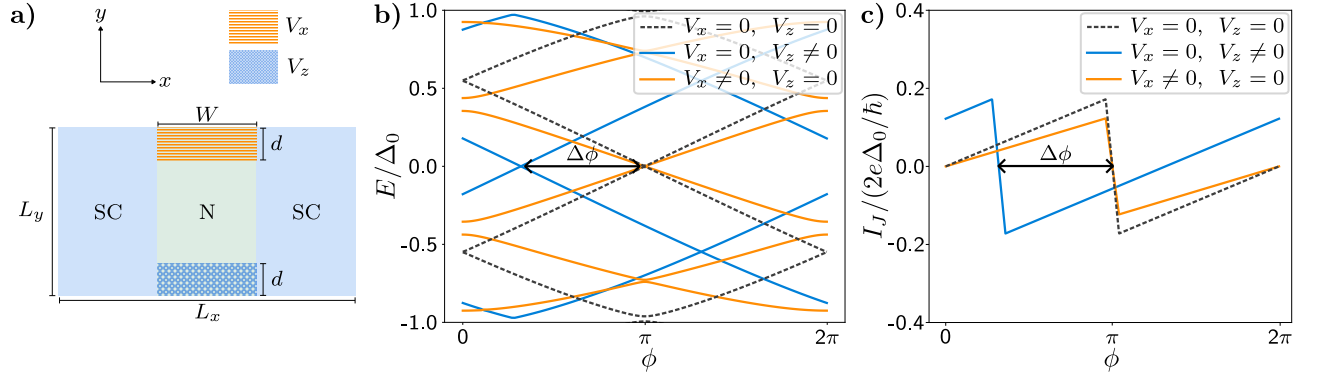


FIG. 2: Josephson junction on a 2D TI. a) Geometry of the junction in our numerical model. Magnetic fields are applied to the edges of the normal region of the junction. b) Single-edge Andreev levels, obtained by setting $V_x = 8\Delta_0, V_z = 0.6\Delta_0$ in a). The dashed line shows the levels under zero field. A V_x field on the edge flattens the levels (orange) whereas a V_z field shifts the levels (blue). c) Single-edge Josephson currents, which account for the total Josephson current calculated from b). A V_x field suppresses the single-edge contribution whereas a V_z field shifts the contribution in ϕ .

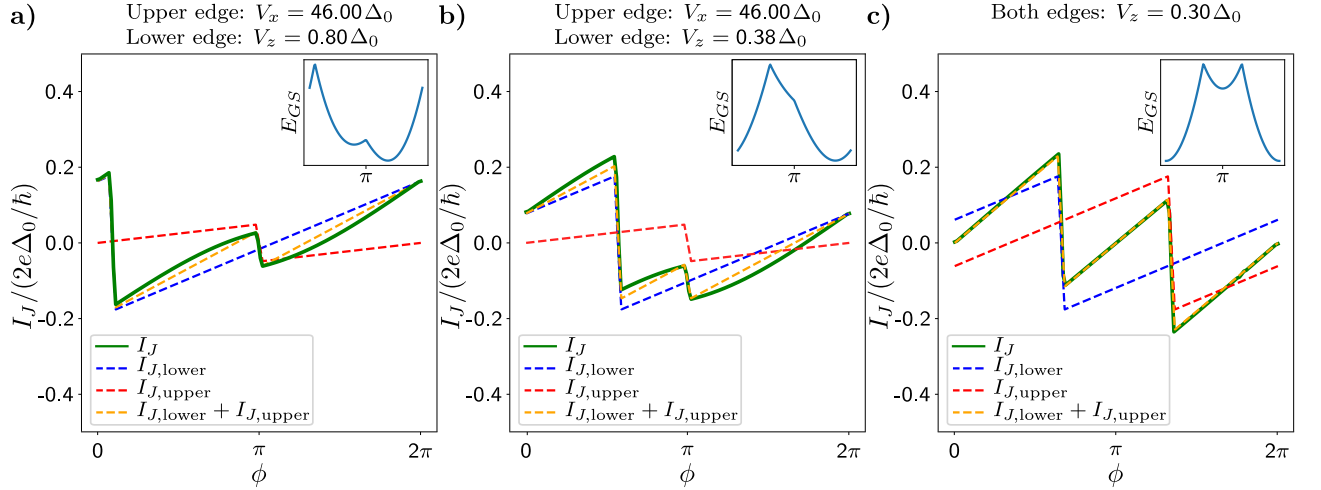


FIG. 3: Josephson current and ground state energy (Josephson potential) of a 2D TI junction with Zeeman fields on the edges. The blue and red lines show the lower and upper edge current modeled by Eq. (7), with an appropriate amount of ϕ -shift and suppression so that their sum (yellow lines) matches the result calculated from Eqs. (4), (5) (green line). The ground state energies calculated from Eq. (5) are shown as insets. a) V_x on the upper edge and V_z on the lower edge, with two stable minima in the ground state energy. If one is able to initialize the phase of the junction at either stable minima, the system will have two critical currents with a large difference. b) V_x on the upper edge and V_z on the lower edge, with one stable minimum in the ground state energy. The system exhibits diode effect. The discrepancy between the linear approximation and the tight-binding result is due to the curvature of the exact $I_{J,\text{single, edge}}(\phi)$ curve, which is eliminated as we move to a longer junction. c) Symmetric V_z on both edges, where the system exhibits no diode effect. The ground state energy has two inequivalent but symmetric minima.

temperature long Josephson junction, the maximum diode efficiency is $(\sqrt{2} - 1)^2 \approx 0.17$, see Fig. 4. An open question is how one can obtain the maximum diode efficiency for a finite-temperature junction of a general length with Zeeman fields on the edges, and the corresponding optimal temperature, junction length, and Zeeman fields; Our preliminary results show that the diode efficiency is generally increased at non-zero temperature. A second open question is whether one can utilize the asymmetric Josephson potential with two minima to obtain highly non-reciprocal critical currents not solely

characterized by η_J .

Upon finalizing this article, we learned of Ref. 69 where a short 2D TI Josephson junction is studied. Other than differences between short and long (our case) junctions, the results seem to agree where there is overlap.

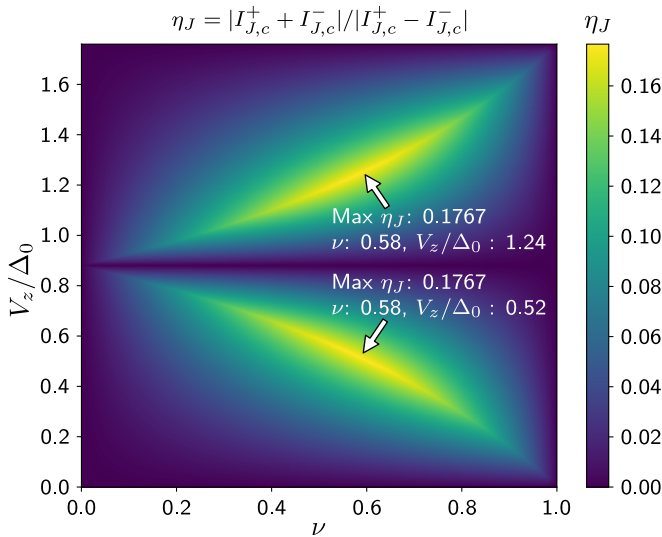


FIG. 4: The Josephson diode efficiency calculated from Eqs. (6), (7), (11), where we take $t = 0.0659$. We assume that Zeeman fields V_x, V_z are applied to top and bottom edges, respectively (see Fig. 2a). The top edge critical current $I_0(V_x)$ is controlled by V_x , parametrized on the horizontal axis by $\nu = 1 - I_0(V_x)/I_0(0)$. The vertical axis shows V_z applied to the bottom edge, leading to a shift (8) to its Josephson current; we take $c = 3.57$. The figure is 2π -periodic in cV_z/Δ_0 . In the limit $t \ll 1$, the analytically calculated maximum diode efficiency is $\max \eta_J = (\sqrt{2} - 1)^2 \approx 0.17$, with $\nu = 2 - \sqrt{2} \approx 0.59$ and $|cV_z/\Delta_0| = (2 - \sqrt{2})\pi, \sqrt{2}\pi$, respectively.

ACKNOWLEDGMENTS

JIV thanks Michael Fuhrer for encouragement and Yuli Lyanda-Geller and Leonid Rokhinson for helpful discussions. This material is based upon work supported by the U.S. Department of Energy, Office of Science, National Quantum Information Science Research Centers, Quantum Science Center.

- ¹M. Nadeem, M. S. Fuhrer, and X. Wang, “The superconducting diode effect,” *Nature Reviews Physics* **5**, 558–577 (2023).
- ²K. Jiang and J. Hu, “Superconducting diode effects,” *Nature Physics* **18**, 1145–1146 (2022).
- ³X. Jiang, P. J. Connolly, S. J. Hagen, and C. J. Lobb, “Asymmetric current-voltage characteristics in type-II superconductors,” *Phys. Rev. B* **49**, 9244–9247 (1994).
- ⁴S. Harrington, J. MacManus-Driscoll, and J. Durrell, “Practical vortex diodes from pinning enhanced yba 2 cu 3 o 7- δ ,” *Applied Physics Letters* **95**, 022518 (2009).
- ⁵D. Y. Vodolazov, A. Y. Aladyshkin, E. Pestov, S. Vdovichev, S. Ustavshikov, M. Y. Levichev, A. Putilov, P. Yunin, A. El’kina, N. Bukharov, *et al.*, “Peculiar superconducting properties of a thin film superconductor-normal metal bilayer with large ratio of resistivities,” *Superconductor Science and Technology* **31**, 115004 (2018).
- ⁶F. Ando, Y. Miyasaka, T. Li, J. Ishizuka, T. Arakawa, Y. Shiota, T. Moriyama, Y. Yanase, and T. Ono, “Observation of superconducting diode effect,” *Nature* **584**, 373–376 (2020).
- ⁷R. Wakatsuki, Y. Saito, S. Hoshino, Y. M. Itahashi, T. Ideue, M. Ezawa,

- Y. Iwasa, and N. Nagaosa, “Nonreciprocal charge transport in noncentrosymmetric superconductors,” *Science advances* **3**, e1602390 (2017).
- ⁸N. F. Q. Yuan and L. Fu, “Supercurrent diode effect and finite-momentum superconductors,” *Proceedings of the National Academy of Sciences* **119** (2022), 10.1073/pnas.2119548119.
- ⁹H. Wu, Y. Wang, Y. Xu, P. K. Sivakumar, C. Pasco, U. Filippozzi, S. S. P. Parkin, Y.-J. Zeng, T. McQueen, and M. N. Ali, “The field-free josephson diode in a van der waals heterostructure,” *Nature* **604**, 653–656 (2022).
- ¹⁰J.-X. Lin, P. Siriviboon, H. D. Scammell, S. Liu, D. Rhodes, K. Watanabe, T. Taniguchi, J. Hone, M. S. Scheurer, and J. I. A. Li, “Zero-field superconducting diode effect in small-twist-angle trilayer graphene,” *Nature Physics* **18**, 1221–1227 (2022).
- ¹¹A. Daido, Y. Ikeda, and Y. Yanase, “Intrinsic Superconducting Diode Effect,” *Phys. Rev. Lett.* **128**, 037001 (2022).
- ¹²S. Ilić and F. S. Bergeret, “Theory of the Supercurrent Diode Effect in Rashba Superconductors with Arbitrary Disorder,” *Phys. Rev. Lett.* **128**, 177001 (2022).
- ¹³J. Díez-Merida, A. Díez-Carlón, S. Yang, Y.-M. Xie, X.-J. Gao, K. Watanabe, T. Taniguchi, X. Lu, K. T. Law, and D. K. Efetov, “Magnetic josephson junctions and superconducting diodes in magic angle twisted bilayer graphene,” *arXiv preprint arXiv:2110.01067* (2021).
- ¹⁴C. Baumgartner, L. Fuchs, A. Costa, S. Reinhardt, S. Gronin, G. C. Gardner, T. Lindemann, M. J. Manfra, P. E. Faria Junior, D. Kochan, *et al.*, “Supercurrent rectification and magnetochiral effects in symmetric josephson junctions,” *Nature nanotechnology* **17**, 39–44 (2022).
- ¹⁵G. P. Mazur, N. van Loo, D. van Driel, J. Y. Wang, G. Badawy, S. Gazibegovic, E. P. A. M. Bakkers, and L. P. Kouwenhoven, “The gate-tunable josephson diode,” (2022).
- ¹⁶C. Baumgartner, L. Fuchs, A. Costa, J. Picó-Cortés, S. Reinhardt, S. Gronin, G. C. Gardner, T. Lindemann, M. J. Manfra, P. F. Junior, *et al.*, “Effect of rashba and dresselhaus spin-orbit coupling on supercurrent rectification and magnetochiral anisotropy of ballistic josephson junctions,” *Journal of Physics: Condensed Matter* **34**, 154005 (2022).
- ¹⁷K. Halterman, M. Alidoust, R. Smith, and S. Starr, “Supercurrent diode effect, spin torques, and robust zero-energy peak in planar half-metallic trilayers,” *Phys. Rev. B* **105**, 104508 (2022).
- ¹⁸A. Daido and Y. Yanase, “Superconducting diode effect and nonreciprocal transition lines,” *Phys. Rev. B* **106**, 205206 (2022).
- ¹⁹T. Karabassov, I. V. Bobkova, A. A. Golubov, and A. S. Vasenko, “Hybrid helical state and superconducting diode effect in superconductor/ferromagnet/topological insulator heterostructures,” *Phys. Rev. B* **106**, 224509 (2022).
- ²⁰H. F. Legg, D. Loss, and J. Klinovaja, “Superconducting diode effect due to magnetochiral anisotropy in topological insulators and rashba nanowires,” *Physical Review B* **106**, 104501 (2022).
- ²¹T. de Picoli, Z. Blood, Y. Lyanda-Geller, and J. I. Väyrynen, “Superconducting diode effect in quasi-one-dimensional systems,” *Phys. Rev. B* **107**, 224518 (2023).
- ²²K. Chen, B. Karki, and P. Hosur, “Intrinsic superconducting diode effects in tilted weyl and dirac semimetals,” *Phys. Rev. B* **109**, 064511 (2024).
- ²³M. Alidoust, C. Shen, and I. Žutić, “Cubic spin-orbit coupling and anomalous Josephson effect in planar junctions,” *Phys. Rev. B* **103**, L060503 (2021).
- ²⁴R. Wakatsuki and N. Nagaosa, “Nonreciprocal current in noncentrosymmetric rashba superconductors,” *Phys. Rev. Lett.* **121**, 026601 (2018).
- ²⁵A. Banerjee, M. Geier, M. Ahnaf Rahman, C. Thomas, T. Wang, M. J. Manfra, K. Flensberg, and C. M. Marcus, “Phase Asymmetry of Andreev Spectra From Cooper-Pair Momentum,” *arXiv e-prints*, arXiv:2301.01881 (2023), arXiv:2301.01881 [cond-mat.supr-con].
- ²⁶N. F. Q. Yuan, “Edelstein effect and supercurrent diode effect,” *arXiv e-prints*, arXiv:2311.11087 (2023), arXiv:2311.11087 [cond-mat.supr-con].
- ²⁷L. Bauriedl, C. Bäuml, L. Fuchs, C. Baumgartner, N. Paulik, J. M. Bauer, K.-Q. Lin, J. M. Lupton, T. Taniguchi, K. Watanabe, *et al.*, “Supercurrent diode effect and magnetochiral anisotropy in few-layer nbse2,” *Nature communications* **13**, 4266 (2022).
- ²⁸S. Y. F. Zhao, X. Cui, P. A. Volkov, H. Yoo, S. Lee, J. A. Gardener, A. J. Akey, R. Engelke, Y. Ronen, R. Zhong, G. Gu, S. Plugge, T. Tummuru, M. Kim, M. Franz, J. H. Pixley, N. Poccia, and P. Kim, “Time-reversal symmetry breaking superconductivity between twisted cuprate superconductors,” *Science* **382**, 1422–1427 (2023).

- ²⁹D. Y. Vodolazov and F. M. Peeters, “Superconducting rectifier based on the asymmetric surface barrier effect,” *Phys. Rev. B* **72**, 172508 (2005).
- ³⁰Y. Hou, F. Nichele, H. Chi, A. Lodesani, Y. Wu, M. F. Ritter, D. Z. Haxell, M. Davydova, S. Ilić, O. Glezakou-Elbert, A. Varambally, F. S. Bergeret, A. Kamra, L. Fu, P. A. Lee, and J. S. Moodera, “Ubiquitous Superconducting Diode Effect in Superconductor Thin Films,” *Phys. Rev. Lett.* **131**, 027001 (2023).
- ³¹A. Burlakov, V. Gurtovoi, A. Il’in, A. V. Nikulov, and V. Tulin, “Superconducting quantum interference device without josephson junctions,” *JETP letters* **99**, 169–173 (2014).
- ³²A. Sundaresh, J. I. Väyrynen, Y. Lyanda-Geller, and L. P. Rokhinson, “Diamagnetic mechanism of critical current non-reciprocity in multilayered superconductors,” *Nature Communications* **14**, 1628 (2023).
- ³³A. Gutfreund, H. Matsuki, V. Plastovets, A. Noah, L. Gorzawski, N. Friedman, G. Yang, A. Buzdin, O. Millo, J. W. A. Robinson, and Y. Anahory, “Direct observation of a superconducting vortex diode,” *Nature Communications* **14** (2023), 10.1038/s41467-023-37294-2.
- ³⁴T. Golod and V. M. Krasnov, “Demonstration of a superconducting diode-with-memory, operational at zero magnetic field with switchable nonreciprocity,” *Nature Communications* **13** (2022), 10.1038/s41467-022-31256-w.
- ³⁵M. Davydova, S. Prembabu, and L. Fu, “Universal Josephson diode effect,” *Science Advances* **8** (2022), 10.1126/sciadv.abo0309.
- ³⁶J. Chiles, E. G. Arnault, C.-C. Chen, T. F. Q. Larson, L. Zhao, K. Watanabe, T. Taniguchi, F. Amet, and G. Finkelstein, “Nonreciprocal Supercurrents in a Field-Free Graphene Josephson Triode,” *Nano Letters* **23**, 5257–5263 (2023).
- ³⁷H. D. Scammell, J. I. A. Li, and M. S. Scheurer, “Theory of zero-field superconducting diode effect in twisted trilayer graphene,” *2D Materials* **9**, 025027 (2022).
- ³⁸S. Banerjee and M. S. Scheurer, “Enhanced Superconducting Diode Effect due to Coexisting Phases,” *Phys. Rev. Lett.* **132**, 046003 (2024).
- ³⁹C.-Z. Chen, J. J. He, M. N. Ali, G.-H. Lee, K. C. Fong, and K. T. Law, “Asymmetric josephson effect in inversion symmetry breaking topological materials,” *Phys. Rev. B* **98**, 075430 (2018).
- ⁴⁰B. Lu, S. Ikegaya, P. Burset, Y. Tanaka, and N. Nagaosa, “Tunable Josephson Diode Effect on the Surface of Topological Insulators,” *Phys. Rev. Lett.* **131**, 096001 (2023).
- ⁴¹T. H. Kikkeler, A. A. Golubov, and F. S. Bergeret, “Field-free anomalous junction and superconducting diode effect in spin-split superconductor/topological insulator junctions,” *Phys. Rev. B* **106**, 214504 (2022).
- ⁴²Y. Zhang, Y. Gu, P. Li, J. Hu, and K. Jiang, “General Theory of Josephson Diodes,” *Phys. Rev. X* **12**, 041013 (2022).
- ⁴³J. Hasan, K. N. Nesterov, S. Li, M. Houzet, J. S. Meyer, and A. Levchenko, “Anomalous Josephson effect in planar noncentrosymmetric superconducting devices,” *Phys. Rev. B* **106**, 214518 (2022).
- ⁴⁴T. Ojanen, “Topological π Josephson junction in superconducting Rashba wires,” *Phys. Rev. B* **87**, 100506 (2013).
- ⁴⁵K. N. Nesterov, M. Houzet, and J. S. Meyer, “Anomalous Josephson effect in semiconducting nanowires as a signature of the topologically nontrivial phase,” *Phys. Rev. B* **93**, 174502 (2016).
- ⁴⁶B. A. Bernevig, T. L. Hughes, and S.-C. Zhang, “Quantum spin hall effect and topological phase transition in hgte quantum wells,” *Science* **314**, 1757–1761 (2006), <https://www.science.org/doi/pdf/10.1126/science.1133734>.
- ⁴⁷C. L. Kane and E. J. Mele, “Quantum Spin Hall Effect in Graphene,” *Phys. Rev. Lett.* **95**, 226801 (2005).
- ⁴⁸C. L. Kane and E. J. Mele, “ Z_2 topological order and the quantum spin hall effect,” *Phys. Rev. Lett.* **95**, 146802 (2005).
- ⁴⁹X. Qian, J. Liu, L. Fu, and J. Li, “Quantum spin Hall effect in two-dimensional transition metal dichalcogenides,” *Science* **346**, 1344–1347 (2014).
- ⁵⁰S. Hart, H. Ren, T. Wagner, P. Leubner, M. Mühlbauer, C. Brüne, H. Buhmann, L. W. Molenkamp, and A. Yacoby, “Induced superconductivity in the quantum spin hall edge,” *Nature Physics* **10**, 638–643 (2014).
- ⁵¹S. Hart, H. Ren, M. Kosowsky, G. Ben-Shach, P. Leubner, C. Brüne, H. Buhmann, L. W. Molenkamp, B. I. Halperin, and A. Yacoby, “Controlled finite momentum pairing and spatially varying order parameter in proximitized hgte quantum wells,” *Nature Physics* **13**, 87–93 (2017).
- ⁵²P. Mandal, S. Mondal, M. P. Stehno, S. Ilić, F. S. Bergeret, T. M. Klapwijk, C. Gould, and L. W. Molenkamp, “Magnetically tunable supercurrent in dilute magnetic topological insulator-based josephson junctions,” *Nature Physics* **1**, 1–7 (2004).
- ⁵³E. Sajadi, T. Palomaki, Z. Fei, W. Zhao, P. Bement, C. Olsen, S. Luescher, X. Xu, J. A. Folk, and D. H. Cobden, “Gate-induced superconductivity in a monolayer topological insulator,” *Science* **362**, 922–925 (2018).
- ⁵⁴V. Fatemi, S. Wu, Y. Cao, L. Bretheau, Q. D. Gibson, K. Watanabe, T. Taniguchi, R. J. Cava, and P. Jarillo-Herrero, “Electrically tunable low-density superconductivity in a monolayer topological insulator,” *Science* **362**, 926–929 (2018).
- ⁵⁵F. Lüpke, D. Waters, S. C. de la Barrera, M. Widom, D. G. Mandrus, J. Yan, R. M. Feenstra, and B. M. Hunt, “Proximity-induced superconducting gap in the quantum spin Hall edge state of monolayer WTe₂,” *Nat. Phys.* **16**, 526–530 (2020).
- ⁵⁶F. Dolcini, M. Houzet, and J. S. Meyer, “Topological Josephson ϕ_0 junctions,” *Phys. Rev. B* **92**, 035428 (2015).
- ⁵⁷S. J. De, U. Khanna, S. Rao, and S. Das, “Quantum spin Hall insulator in proximity with a superconductor: Transition to the Fulde-Ferrell-Larkin-Ovchinnikov state driven by a Zeeman field,” *Phys. Rev. B* **108**, L161403 (2023).
- ⁵⁸L. Vigliotti, F. Cavaliere, G. Passetti, M. Sasseti, and N. Traverso Ziani, “Reconstruction-Induced ϕ_0 Josephson Effect in Quantum Spin Hall Constrictions,” *Nanomaterials* **13**, 1497 (2023).
- ⁵⁹J. Wang, Y. Jiang, J. J. Wang, and J.-F. Liu, “Efficient Josephson diode effect on a two-dimensional topological insulator with asymmetric magnetization,” *Phys. Rev. B* **109**, 075412 (2024).
- ⁶⁰A. M. Black-Schaffer and J. Linder, “Magnetization dynamics and Majorana fermions in ferromagnetic Josephson junctions along the quantum spin Hall edge,” *Phys. Rev. B* **83**, 220511 (2011).
- ⁶¹C. W. Groth, M. Wimmer, A. R. Akhmerov, and X. Waintal, “Kwant: a software package for quantum transport,” *New Journal of Physics* **16**, 063065 (2014).
- ⁶²Our code to reproduce the figures is available at <https://purrr.purdue.edu/publications/4493/1>.
- ⁶³M. Tinkham, *Introduction to Superconductivity* (Dover Publications, 2004).
- ⁶⁴C. W. J. Beenakker, D. I. Pikulin, T. Hyart, H. Schomerus, and J. P. Dahlhaus, “Fermion-Parity Anomaly of the Critical Supercurrent in the Quantum Spin-Hall Effect,” *Phys. Rev. Lett.* **110**, 017003 (2013).
- ⁶⁵L. Fu and C. L. Kane, “Josephson current and noise at a superconductor/quantum-spin-Hall-insulator/superconductor junction,” *Phys. Rev. B* **79**, 161408 (2009).
- ⁶⁶J. I. Väyrynen, G. Rastelli, W. Belzig, and L. I. Glazman, “Microwave signatures of majorana states in a topological josephson junction,” *Phys. Rev. B* **92**, 134508 (2015).
- ⁶⁷The critical current can however⁶⁸ differ significantly, depending on which minimum the system is initialized in.
- ⁶⁸E. Goldobin, D. Koelle, R. Kleiner, and A. Buzdin, “Josephson junctions with second harmonic in the current-phase relation: Properties of ϕ junctions,” *Phys. Rev. B* **76**, 224523 (2007).
- ⁶⁹S. Fracassi, S. Traverso, N. Traverso Ziani, M. Carrega, S. Heun, and M. Sasseti, “Anomalous supercurrent and diode effect in locally perturbed topological Josephson junctions,” *arXiv e-prints*, arXiv:2403.17894 (2024), arXiv:2403.17894 [cond-mat.supr-con].